Acta Oceanol. Sin., 2019, Vol. 38, No. 4, P. 126–135
https://doi.org/10.1007/s13131-019-1418-2
http://www.hyxb.org.cn
E-mail: hyxbe@263.net

Classification and 3-D distribution of upper layer water masses in the northern South China Sea

Jia Zhu[1], Quanan Zheng[2], Jianyu Hu[1]*, Hongyang Lin[1], Dewen Chen[3], Zhaozhang Chen[1], Zhenyu Sun[1], Liyan Li[1], Hao Kong[4]

[1] State Key Laboratory of Marine Environmental Science, College of Ocean and Earth Sciences, Xiamen University, Xiamen 361102, China

[2] Department of Atmospheric and Oceanic Science, University of Maryland, College Park, Maryland 20742, USA

[3] Marine Forecast Station of Xiamen, State Oceanic Administration, Xiamen 361012, China

[4] Fujian Provincial Key Laboratory of Coast and Island Management Technology, Fujian Institute of Oceanography, Xiamen 361013, China

Received 10 February 2018; accepted 14 May 2018

Abstract

Using the fuzzy cluster analysis and the temperature-salinity (T-S) similarity number analysis of cruise conductivity-temperature-depth (CTD) data in the upper layer (0–300 m) of the northern South China Sea (NSCS), we classify the upper layer water of the NSCS into six water masses: diluted water (D), surface water (SS), the SCS subsurface water mass (U_S), the Pacific Ocean subsurface water mass (U_P), surface-subsurface mixed water (SU) and subsurface-intermediate mixed water (UI). A new stacked stereogram is used to illustrate the water mass distribution, and to examine the source and the distribution of U_P, combining with the sea surface height data and geostrophic current field. The results show that water mass U_P exists in all four seasons with the maximum range in spring and the minimum range in summer. In spring and winter, the U_P intrudes into the Luzon Strait and the southwest of Taiwan Island via the northern Luzon Strait in the form of nonlinear Rossby eddies, and forms a high temperature and high salinity zone east of the Dongsha Islands. In summer, the U_P is sporadically distributed in the study area. In autumn, the U_P is located in the upper 200 m layer east of Hainan Island.

Key words: water mass classification, northern South China Sea, fuzzy cluster analysis, T-S similarity number

Citation: Zhu Jia, Zheng Quanan, Hu Jianyu, Lin Hongyang, Chen Dewen, Chen Zhaozhang, Sun Zhenyu, Li Liyan, Kong Hao. 2019. Classification and 3-D distribution of upper layer water masses in the northern South China Sea. Acta Oceanologica Sinica, 38(4): 126–135, doi: 10.1007/s13131-019-1418-2

1 Introduction

The water mass distribution is a basic property of the ocean. Compared with water masses in the deep ocean, the water masses in the shelf water are poor in uniformity and stability. Since the 1960s, water mass analysis methods have been developed for shallow water, for example, the quantitative analysis of the temperature-salinity (T-S) relationship (Mao et al., 1964), the systematic cluster analysis (Su et al., 1983; Li et al., 1983), the stepwise cluster analysis (Qiu et al., 1984), the fuzzy cluster analysis (Chen and Du, 1990; Li et al., 1992; Yang et al., 1992), and the T-S diagram method (Zou et al., 2000).

The South China Sea (SCS) is a semi-enclosed marginal sea of the Northwest Pacific. Thus, its water masses are characterized by complex 3-D structure and seasonal variability because of the Pacific water intrusion, rich river run off, monsoon wind forcing and complicated basin topography. Previous investigators have conducted the water mass analysis in the SCS (Wyrtki, 1961; Nitani, 1972; Dietrich et al., 1980) and in the northern SCS (NSCS; Li et al., 1983; Li and Su, 1989; Li et al., 1989a, b). Liu et al. (2001) classified the summer SCS water into nine water masses using four different analysis methods, and compared their distributions. On the basis of observations during summer and winter cruises in 1998, Li et al. (2002a, b) differentiated the SCS water into six water masses: the surface water (SS), the subsurface water (U), the subsurface-intermediate mixed water (UI), the intermediate water, the deep water and the bottom water, using cluster analysis, discriminant analysis and fuzzy analysis methods. Zhu and Ji (2002) classified the summer SCS water into five water masses: SS, U, the intermediate water, the deep water and the bottom water, using Q-type multidimensional cluster analysis. Tian and Wei (2005) divided the water masses in the NSCS and the Luzon Strait into SS, U, the intermediate water and the deep water. Liu et al. (2008) analyzed the annual and seasonal variation characteristics of SS and the intermediate water. Cheng et al. (2014) classified the NSCS water into five water masses: the near shore mixed water, SS, U, the intermediate water and the deep water using fuzzy analysis.

In summary, the previous studies classified the SCS water masses, but their 3-D distributions and seasonal variability remain unclear. In particular, the role on how the Pacific water mass plays in the water mass formation in the SCS is lacking of

Foundation item: The National Natural Science Foundation of China under contract No. 41776027; the National Basic Research Program of China under contract Nos 2015CB954004 and 2009CB421208; the Open Fund of the Key Laboratory of Ocean Circulation and Waves, Chinese Academy of Sciences under contract No. KLOCW1808.
*Corresponding author, E-mail: hujy@xmu.edu.cn

research.

In this study, on the basis of the CTD data observed in the upper 300 m in the NSCS during four season cruises, we classify the water masses using the fuzzy cluster analysis method. Then we use the *T*-*S* water similarity method to define the water mass boundaries, and divide the U mass into the SCS U mass (U_S) and the Pacific U mass (U_P). The distribution range of the U_P and its influence on the formation of water masses in the NSCS are examined.

2 Data and methods

2.1 *Data*

In this study, we focus on the analysis of the *T*-*S* data in the NSCS covering a region from 17° to 26°N and from 108° to 124°E. Cruise observations were carried out on board the R/V *Dongfanghong 2* in four seasons from 2009 to 2011, using SBE911 or SBE917 plus CTD profiler manufactured by the Sea Bird Corporation. There were total 284 stations, i.e., 92 in spring, 79 in summer, 47 in autumn and 66 in winter as shown in Fig. 1.

2.2 *Data preprocessing method*

To speed up the matrix calculation and show clearly the distribution of the water masses, we focus on the *T* and *S* data observed in the upper 300 m only. The vertical resolution of the CTD data is 1 m.

In order to balance the *T*-*S* ratio, the data were standardized by the extreme value:

$$x_{ik} = \frac{x^*_{ik} - \min(x^*_{ik})}{\max(x^*_{ik}) - \min(x^*_{ik})}, \quad i = 1, 2, ..., N, \quad k = 1, 2, ..., M, \quad (1)$$

where *N* is the number of samples, *M* is the number of parameters (*M*=2, *T* and *S*), and x^*_{ik} is the data value before standardization.

2.3 *Fuzzy cluster analysis method*

The details of fuzzy cluster analysis method refer to Li et al. (1989a).

2.3.1 *Basic principle*

Suppose *X* is a definite universe representing the studied sea area with *m* samples,

$$X = \{\vec{x}_1, \vec{x}_2, ..., \vec{x}_m\}. \quad (2)$$

The sample $\vec{x}_i$, $i = 1, 2, ..., m$, can be specified by *n* quantitative indexes, such as temperature, salinity, etc. Thus, the *i*th sample can be written as

$$\vec{x}_i = (x_{i1}, x_{i2}, ..., x_{in}) \quad (3)$$

corresponding to a point in the *n*-dimensional space of index.

We use the scalar method on the basis of Euclidean distance. The formula is

$$r_{ij} = \frac{1}{D^2_{ij} + 1}, \quad (4)$$

where D^2_{ij} is the Euclidean square distance,

$$D^2_{ij} = (\vec{x}_i - \vec{x}_j)(\vec{x}_i - \vec{x}_j)' = \sum_{k=1}^{m}(x_{ik} - x_{jk})^2, \quad i, j = 1, 2, ..., m. \quad (5)$$

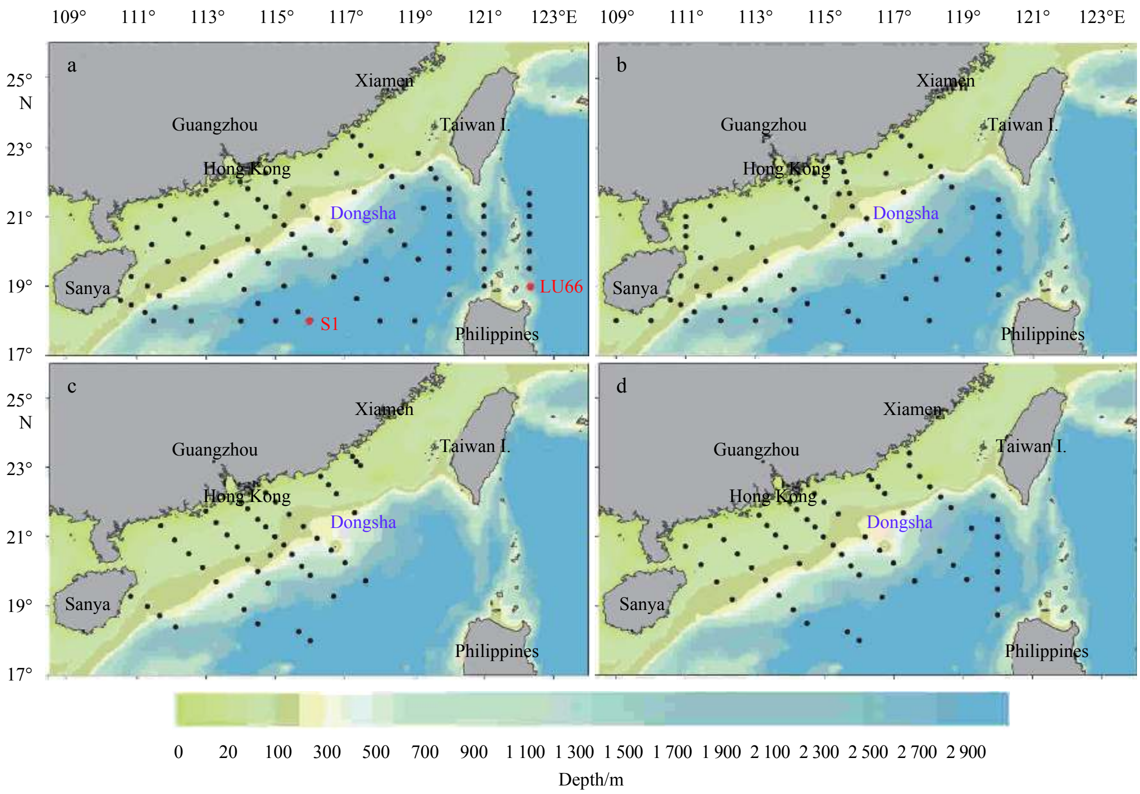

Fig. 1. Cruise sections and CTD stations in the NSCS from 2009 to 2011. a. Spring, b. summer, c. autumn and d. winter.

From Eq. (4), a fuzzy similar relation $\underset{\sim}{R}$ is established as

$$\underset{\sim}{R} = [r_{ij}], \quad i,j = 1, 2, ..., m.$$

Obviously, $\underset{\sim}{R}$ is reflexive and symmetric but not necessarily transitive. The transitivity of $\underset{\sim}{R}$ can be realized by compound-calculation.

2.3.2 *Determination of the number of water masses*

The divided number of water masses is different when different λ-values are taken for the same batch of samples. The approach presented here is to control the λ-values so that it would increase gradually in fuzzy cluster procedure so as to make m samples be divided into $2, 3, 4, ...$ water masses in order. At the same time, we use F-test to each cluster scheme and choose the optimal one with the maximum F-value from significant options, by which the number of water masses is determined. The calculating formula of F-value is

$$F = \frac{\dfrac{1}{n(T-1)}\displaystyle\sum_{i=1}^{T} m_i (V_i - \vec{x})(V_i - \vec{x})'}{\dfrac{1}{n(m-T)}\displaystyle\sum_{i=1}^{T}\sum_{j\in i\text{th-water-mass}} (\vec{x}_j - V_j)(\vec{x}_j - V_j)'}, \tag{6}$$

where T denotes the number of water masses, and m_i is the number of the samples merged into the ith water mass,

$$V_i = (v_{i1}, v_{i2}, ..., v_{in}), \tag{7}$$

the cluster center of the ith water mass and its component

$$v_{ik} = \frac{1}{m_i}\sum_{j\in i\text{th-water-mass}} x_{jk}, \quad k = 1, 2, ..., n, \tag{8}$$

with $\vec{x}$ being the average of the global samples of X.

3 Results

3.1 *Results from fuzzy cluster analysis*

Applying the fuzzy cluster analysis method to the upper layer water (0–300 m) of the NSCS yields five water masses: the diluted water (D), the surface water (SS), the surface-subsurface mixed water (SU), the subsurface water (U) and the subsurface-intermediate mixed water (UI). The classification results for the four seasons are shown in Fig. 2. One can see that the surface layer is covered by the SS in spring and summer. D is distributed mainly in the area near the Zhujiang (Pearl) River Estuary, and its distribution range and depth are larger in autumn and winter than those in spring and summer. U is distributed mainly in the 80–200 m layer with high salinity. The distribution range of U is the largest in spring, occupying the 50–200 m layer, and the dis-

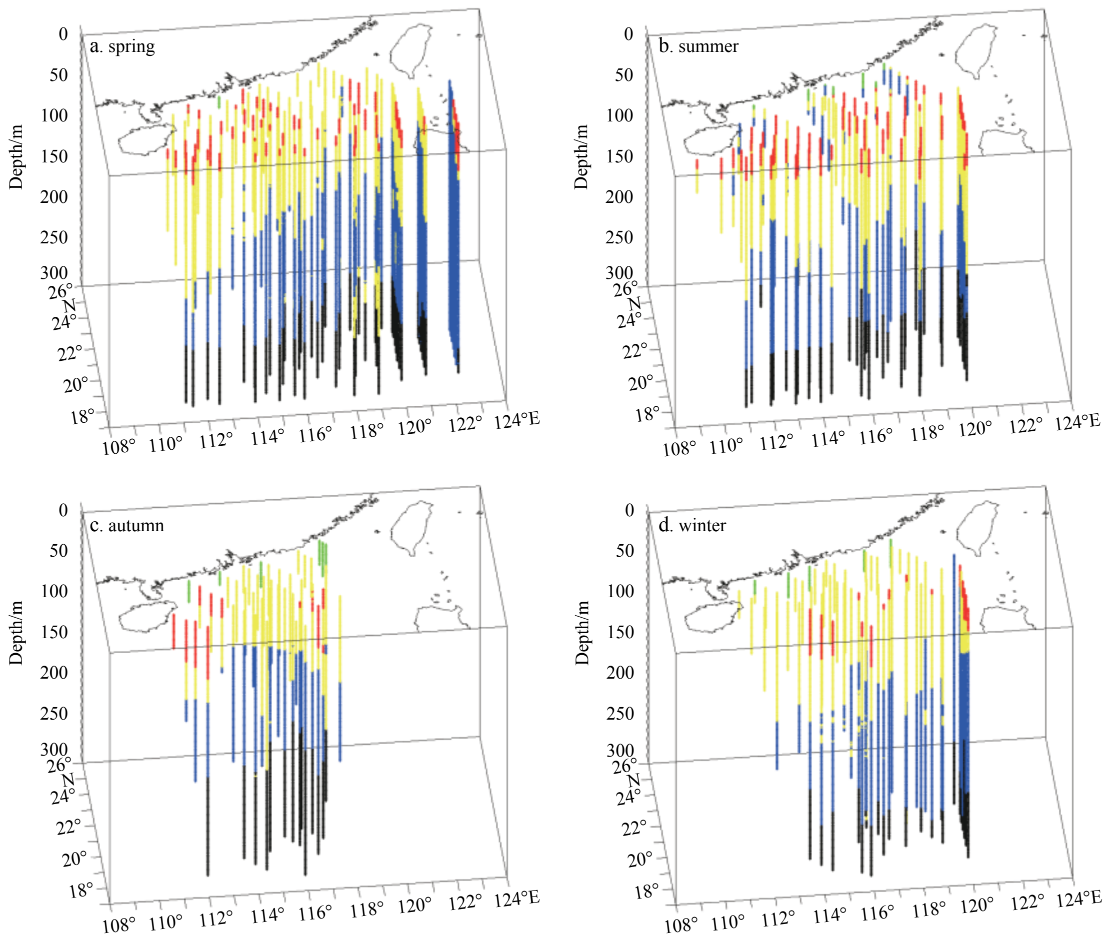

Fig. 2. Classification results of upper layer water masses in the NSCS. Green: diluted water, red: surface water, yellow: surface-subsurface mixed water, blue: subsurface water, and black: subsurface-intermediate mixed water.

tribution range mainly in the 70–200 m is the second in summer and winter. SU is distributed mainly in the 50–150 m layer in spring and summer, and appears in most of the stations from the surface to the 100 m layer in autumn and winter. UI is distributed below 250 m with the stable distribution range and properties.

3.2 *T-S similarity number*

The results of the fuzzy cluster or systematic cluster analysis give a qualitative output, 1 or 0, or yes or no, for water mass that the water sample belongs to. However, a water sample would not absolutely belong to one water mass. Instead, it may be a mixture of two or even more water masses, having the characteristics of a multiple water mass. In order to present a more realistic distribution of water masses, we defined a *T-S* similarity number (TSSN) to further quantify the water sample by clearly specifying the boundaries between the water masses.

The TSSN or Γ can be considered as the similarity between a random water sample point and a typical water mass, ranging from 0 to 1. As shown in Fig. 3, X represents a water sample, AB is an intersection of the isopycnal line, at which X is located. Parameter Γ is defined as

$$\Gamma = \frac{D_{\rm A}}{D_{\rm A}+D_{\rm B}}\ (0\leqslant\Gamma\leqslant 1), \tag{9}$$

where $D_{\rm A}$ and $D_{\rm B}$ are the distances from X to the *T-S* curves of Types A and B water masses along the isopycnal line, respectively,

$$D_{\rm A} = \int_{S_{\rm A}}^{S_{\rm X}} \sqrt{1+\left(\frac{{\rm d}T}{{\rm d}S}\right)^2}\,{\rm d}S \tag{10}$$

and

$$D_{\rm B} = \int_{S_{\rm X}}^{S_{\rm B}} \sqrt{1+\left(\frac{{\rm d}T}{{\rm d}S}\right)^2}\,{\rm d}S, \tag{11}$$

where integral limits $S_{\rm A}$, $S_{\rm B}$ and $S_{\rm X}$ are the salinity at A, B and X.

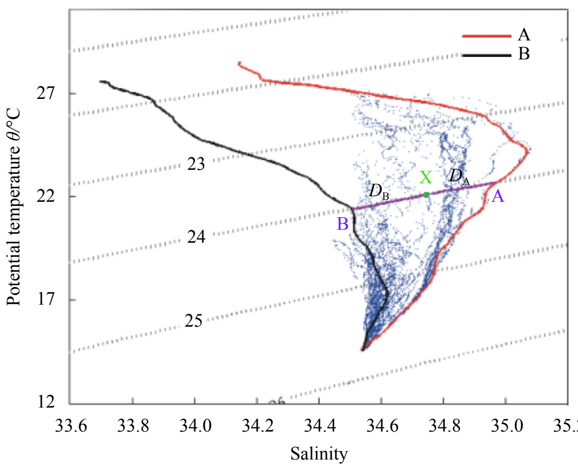

Fig. 3. Schematic diagram for calculating the *T-S* similarity number of water samples. Red and black lines represent *T-S* curves of Types A and B water masses, respectively. Blue dots are *T-S* values of the subsurface water samples taken during the spring cruise.

The closer the value of Γ is to 0, the higher the similarity of the X water sample to Type A water mass. The closer the value of Γ is to 1, the higher similarity of the X water sample to the Type B water mass. We considered Γ=0.5 to be a boundary line between Types A and B water masses.

3.3 *Classification results of the subsurface water mass*

Based on the classification results in Section 3.1, we note that the U is distributed mainly in the 80–200 m layer. We set the Pacific water as Type A water, and the SCS water as Type B water. Specifically, the *T-S* curve at Sta. LU66 (Fig. 1a), where the Kuroshio passes through, represents the typical curve of Type A water mass, and the *T-S* curve at Sta. S1 (Fig. 1a) represents the typical curve of Type B water mass (Du et al., 2013). Thus, from TSSN distribution figures, one can see that the subsurface water (U) in the 80–200 m layers could be classified into the $\rm U_P$ (with a similarity<0.5) and the $\rm U_S$ (with a similarity>0.5).

Figures 4–7 show the TSSN contribution of the $\rm U_P$ and $\rm U_S$ in spring, summer, autumn and winter, respectively. In spring, the boundary line of the $\rm U_P$ and $\rm U_S$ is located in the Luzon Strait at 50 m. At 100–150 m, the $\rm U_P$ is distributed sporadically in the SCS basin west of 120°E. At 175 m, the intrusion of the $\rm U_P$ reaches its largest range in the SCS, from the north of Dongsha Island even to the south of (18°N, 115°E). At 200 m, the $\rm U_P$ intrudes into the SCS via the northern Luzon Strait, reaching 118.5°E. In the southern Luzon Strait, the $\rm U_P$ is confined to 121.3°E.

In summer, the region is completely occupied by the $\rm U_S$ at 50 m and 125–150 m. At 100 m, the $\rm U_P$ appears in the middle Luzon Strait near (20°N, 119°E). At 175 and 200 m, the $\rm U_P$ appears to the east of Hainan Island, and is distributed sporadically at 115°E, 118°E and 120°E.

In autumn, the water properties at 50–150 m belong to the $\rm U_S$. At 175 m, the $\rm U_P$ is distributed in a range from 114° to 119°E south of 19°N. At the 200 m layer, the $\rm U_P$ expands eastward from the Hainan Island to 116°E.

In winter, the $\rm U_P$ intrudes into the SCS to 118.5°E via the northern Luzon Strait at 50 m. It has no trace at 100 m, but appears again at 125 m, showing a westward water tongue to the SCS via the northern Luzon Strait. At 150 and 175 m, it enters the SCS from the northern and middle Luzon Strait as a water tongue reaching the central basin. At 200 m, it is distributed in a range from 20° to 22°N, and from 117° to 119°E, forming a high temperature and high salinity region.

4 NSCS upper layer water mass classification

Based on the results of fuzzy cluster and TSSN analysis, we classify the upper layer water of the NSCS into six water masses: the diluted water (D), the surface water (SS), the SCS subsurface water mass ($\rm U_S$), the Pacific subsurface water mass ($\rm U_P$), the surface-subsurface mixed water (SU) and the subsurface-intermediate mixed water (UI). In order to display the structure of the water masses more intuitively, a new stacked stereogram is used to illustrate the water mass distribution, as shown in Fig. 8. The core *T-S* values of these water masses in the four seasons are listed in Table 1.

As shown in Fig. 8a, in spring the D is distributed near the Zhujiang River Estuary with a small range and low salinity. The core salinity of D is 29.17 with the lowest salinity of 23.60. The SS is distributed in the offshore region with depths shallower than 20 m, including the surface of the Luzon Strait. The core temperature and salinity are 28.24°C and 33.80, respectively. The $\rm U_S$ is concentrated mainly at 100–250 m in the basin region of the NSCS. The core temperature and salinity values of the $\rm U_S$ are

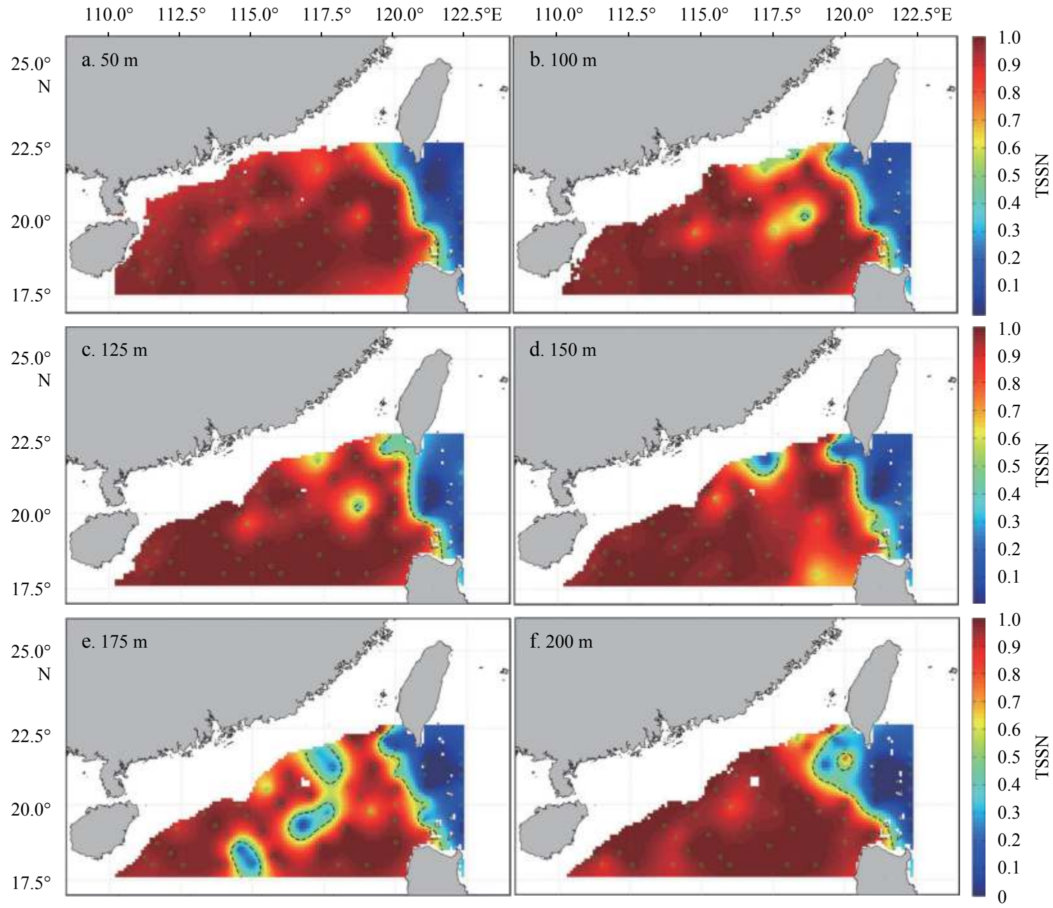

Fig. 4. TSSN contribution of the SCS and the Pacific subsurface water masses in spring.

17.86°C and 34.55. The U_P with high temperature and salinity values is observed at 50–300 m in the Luzon Strait and its adjacent area. The core temperature and salinity values are 21.06°C and 34.79. At 50–100 m, the boundary between the U_P and U_S extends from the southwest of Taiwan to the central coast of Luzon Island. At 150–200 m, the U_P intrudes into the NSCS even to the north of Dongsha Island via the northern Luzon Strait. At 250–300 m, the boundary between the U_S and U_P moves back to the Luzon Strait. The SU is distributed from the surface to 150 m, while the UI is located below 250 m only. The water mass struc-

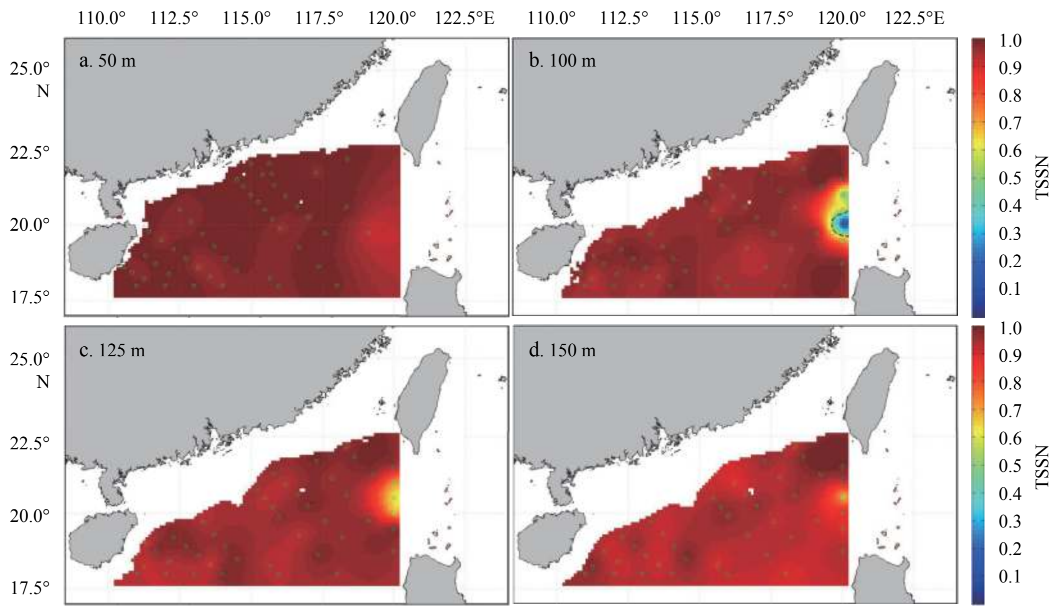

Fig. 5

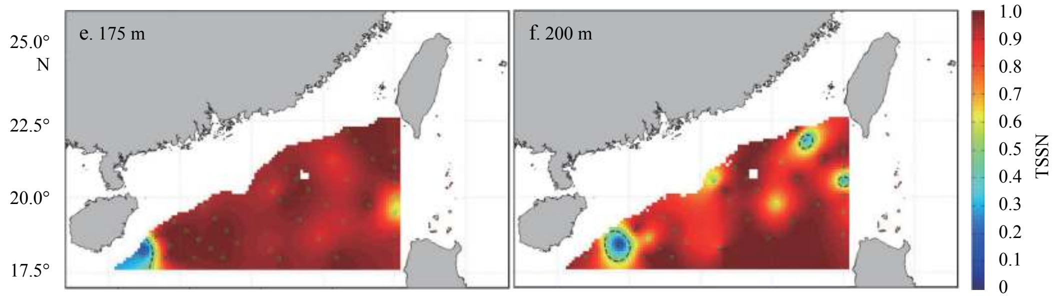

Fig. 5. TSSN contribution of the SCS and the Pacific subsurface water masses in summer.

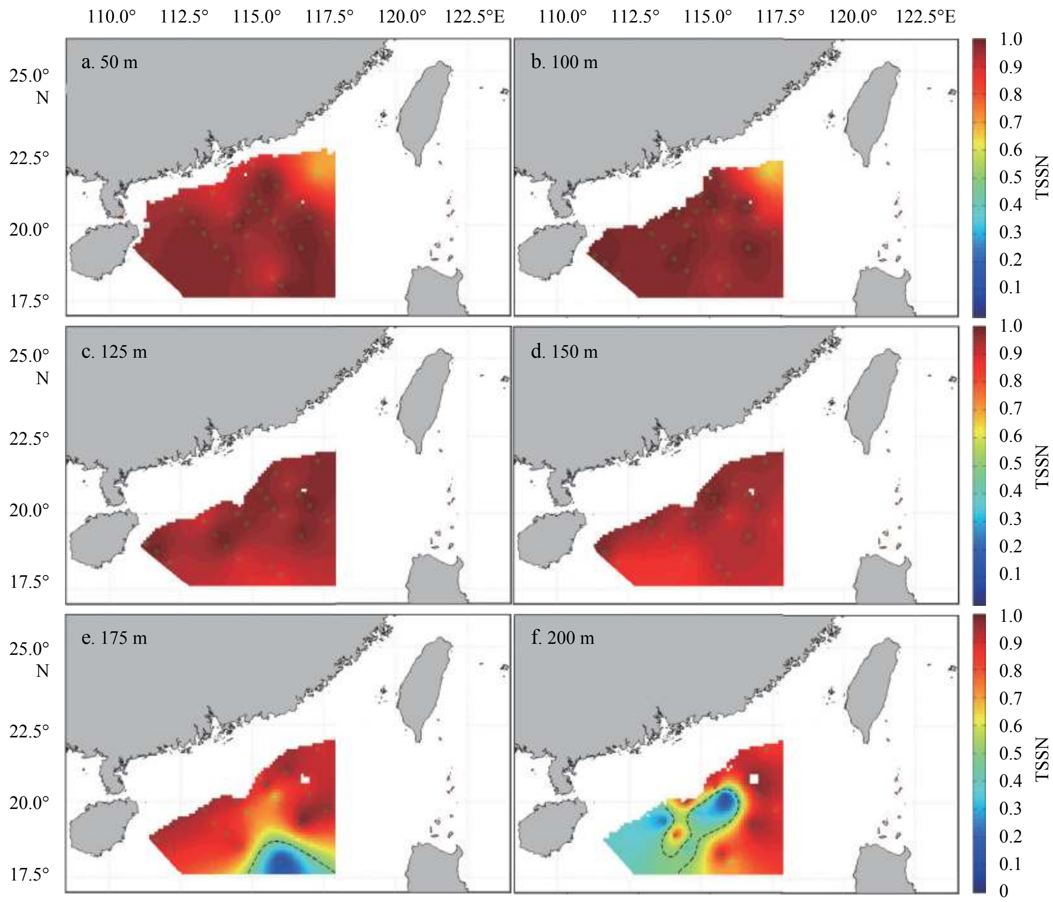

Fig. 6. TSSN contribution of the SCS and the Pacific subsurface water masses in autumn.

ture of the Luzon Strait can be seen as four layers: 2–20 m is occupied by the SS, 20–100 m is shared by the SU and the U_P, 100–200 m is almost divided equally between the U_S and the U_P, and 200–300 m is shared by the UI and the U_P.

The D extends to a narrow strip along the coast of Guangdong, China under the influence of the southwesterly monsoon in summer (Fig. 8b). Influenced by the strong solar radiation, the SS is distributed at the offshore stations from the surface to 50 m, with a core temperature of 29.43°C. Coastal upwelling related to the U_S, as a characteristic water body in summer, is located to the east of Hainan Island and the coast of Guangdong, from bottom to surface. The U_S also occupies the offshore stations from 100 to 200 m, and the core values of temperature and salinity are 18.31°C and 34.49. The U_P is scattered around 100 and 200 m with a core salinity value of 34.69 higher than that in spring and winter. The SU can be observed from the surface to 100 m, while the UI is located below 250 m only.

In autumn, the D extends in two directions from the Zhujiang River Estuary northeastward to Dongshan, Fujian, and southwestward to the east of the Leizhou Peninsula, Guangdong (Fig. 8c). The core values of temperature and salinity are 21.69°C and 31.91. The SS is distributed in the shallow water of the eastern Hainan Island. Because the study region experienced several strong winds during the cruise, the water was well mixed, so that the SU is present from the surface to 175 m. The U_S occupies most the layers from 100 to 200 m, while the U_P is distributed in the south of the study region at 175 m and the west at 200 m. The UI is located below 200 m, characterized by stable temperature

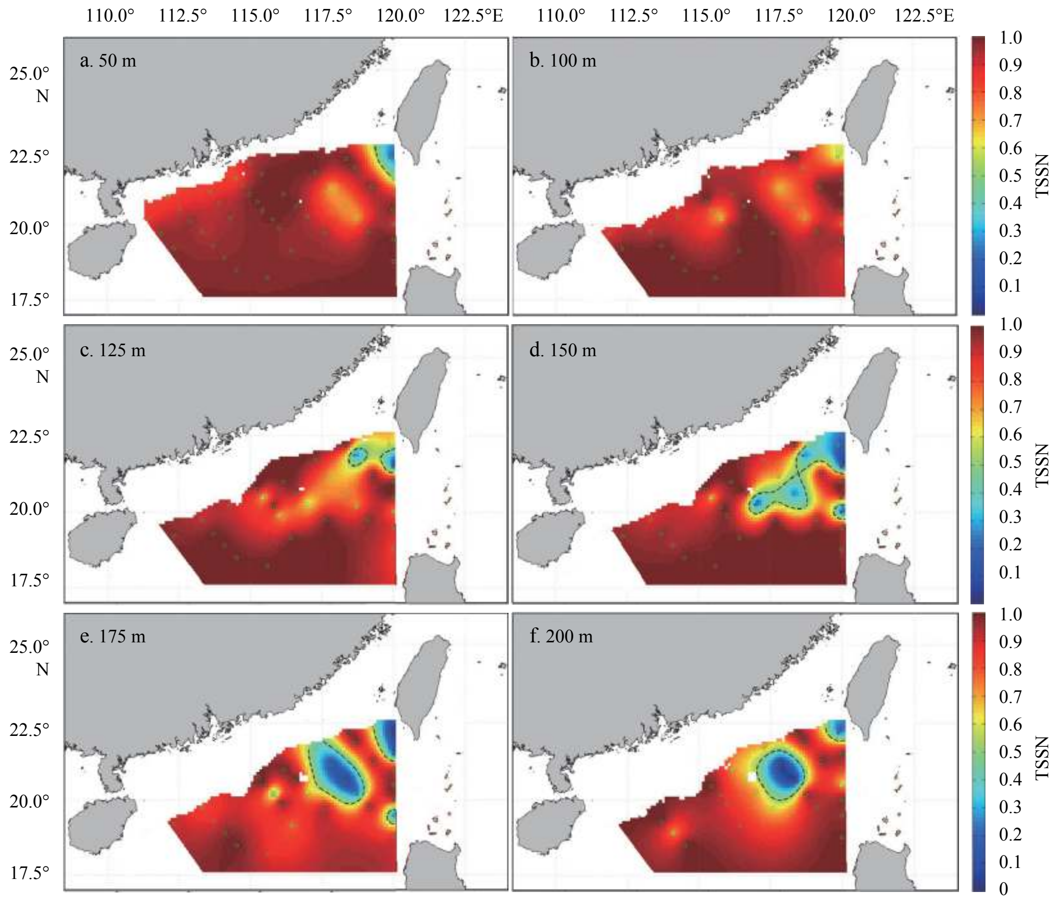

Fig. 7. TSSN contribution of the SCS and the Pacific subsurface water masses in winter.

and salinity.

In winter, forced by the northeasterly monsoon, the D spreads southward from the Zhujiang River Estuary and forms a narrow strip (Fig. 8d). The core values of temperature and salinity are 17.19°C and 32.29. The SS is distributed at the surface in the southern most of the NSCS. The U_S can be found at 50–300 m, and is most broadly distributed at 100–200 m, with core temperature and salinity values of 17.66°C and 34.57. The U_P intrudes into the NSCS via the northern Luzon Strait at 150–250 m, appears to the southwest of Taiwan at 20–50 m, and forms a small area of high salinity in the basin at 175–200 m. The core values of temperature and salinity are 19.93°C and 34.71. The SU is mainly distributed from the surface to 100 m, while the UI remains stable below 250 m.

5 Discussion

As shown in Fig. 4, the U_P is broadly distributed in the adjacent area of the Luzon Strait at 20–250 m in spring. Based on the spring average satellite altimeter absolute dynamic topography and the corresponding geostrophic current during the cruise periods as shown in Fig. 9, the geostrophic current in the Luzon Strait is westward in the north and eastward in the south of the strait. The subsurface water enters the NSCS from the northern Luzon Strait and exits from the south, corresponding to the U_P distribution pattern, which is wide in the north and narrow in the south. The surface geostrophic currents show no remarkable signature for the Pacific water entering the SCS in summer. In autumn, the surface geostrophic current field (GCF) shows a branch of the Kuroshio entering the SCS from the northern Luzon Strait, and flowing southwestward along the continental slope of the SCS, as far as to the east of Hainan Island. This would be the source of the U_P, which appears in the east of Hainan Island at 200 m as shown in Figs 6g and 8c. In winter, the GCF in the Luzon Strait shows that the Kuroshio intrudes into the NSCS through the Luzon Strait, forming an anti-cyclonic eddy to the east of Dongshan. Its location matches the high temperature and high salinity region around 20–22°N, 117–119°E, where the U_P is distributed.

Figures 4 and 7 indicate that at 175 m in spring and 150 m in winter, the U_P presents a distribution pattern with several continuously distributed eddies, which would be the signature of the nonlinear Rossby eddies originating from the Pacific and entering the NSCS through the Luzon Strait (Hu et al., 2012; Xie et al., 2016, 2017; Zheng et al., 2011, 2017). Those water masses with the Pacific Ocean *T-S* characteristics continuously mix with the SCS water masses during their westward propagation process along the continental shelf, so that the original characteristics are gradually weakened.

6 Conclusions

In this study, the upper layer water (shallower than 300 m) of the NSCS is classified into six water masses: the diluted water (D), the surface water (SS), the SCS subsurface water mass (U_S), the Pacific subsurface water mass (U_P), the surface-subsurface mixed water (SU) and the subsurface-intermediate mixed water (UI) using fuzzy cluster and TSSN analysis methods. The 3-D distribu-

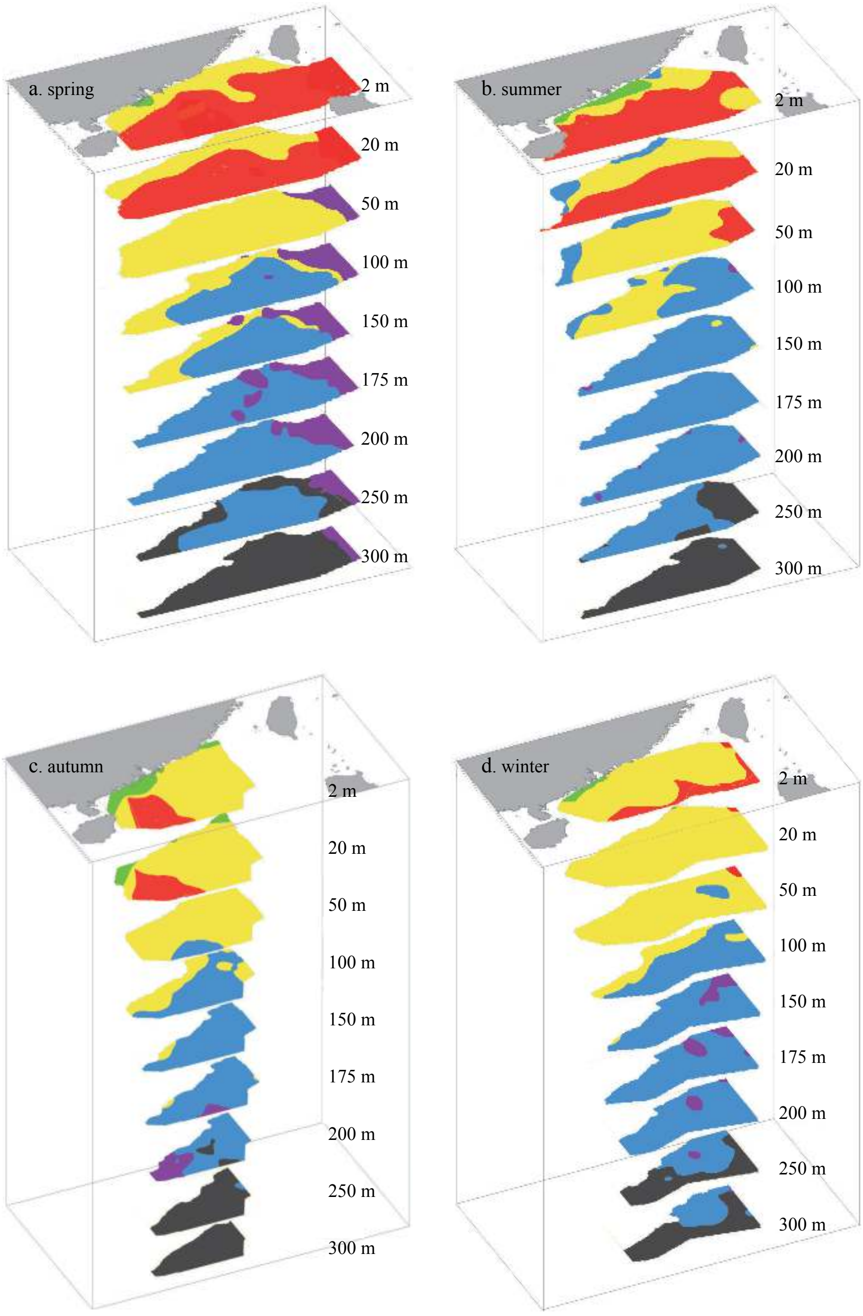

Fig. 8. Water mass classification in the NSCS. a. Spring, b. summer, c. autumn and d. winter. Green: diluted water (D); red: surface water (SS); yellow: surface-subsurface mixed water (SU); blue: SCS subsurface water (U_S); violet: Pacific subsurface water (U_P); and black: subsurface-intermediate mixed water (UI).

tion characteristics and formation mechanisms are analyzed, combining the SSH and GCF during four cruise periods. The major results are summarized as follows:

(1) The distribution ranges of the Zhujiang River diluted water D in summer and autumn are relatively large. Forced by the southwesterly monsoon, The D extends to a narrow region along the coast of Guangdong, China in summer. It extends in two directions, northeastward to Dongshan and southwestward to the east of the Leizhou Peninsula in autumn. It becomes a narrow southward strip in winter and spring.

(2) The surface water SS is mainly distributed above 20 m and 50 m at the offshore stations in spring and summer. Its distribution ranges in autumn and winter are relatively small, in the shallow water of eastern Hainan Island and at the surface in the southern most of the NSCS, respectively.

(3) The SCS subsurface water mass U_S is mainly concentrated at 100–250 m at the offshore stations in the four seasons. In summer, it exists at 20–100 m to the east of Hainan Island and the coastal water region of Guangdong in the form of coastal upwelling.

(4) The Pacific subsurface water mass U_P is observed in the four seasons, having the largest distribution in spring and the smallest in summer. In spring and winter the U_P intrudes into the NSCS through the Luzon Strait in the form of nonlinear Rossby

Table 1. The core *T* and *S* values of the water masses in the upper water of the NSCS

Season		Diluted water (D)	Surface water (SS)	SCS subsurface water (U_S)	Pacific subsurface water (U_P)	Surface-subsurface mixed water (SU)	Subsurface-intermediate mixed water (UI)
Spring	*T*/°C	26.55	28.24	17.86	21.06	21.39	12.84
	S	29.17	33.80	34.55	34.79	34.31	34.48
Summer	*T*/°C	29.28	29.43	18.31	20.43	22.87	13.34
	S	31.23	33.39	34.49	34.69	34.16	34.51
Autumn	*T*/°C	21.69	27.38	17.94	18.51	22.62	13.21
	S	31.91	33.43	34.47	34.54	34.06	34.49
Winter	*T*/°C	17.19	24.78	17.66	19.93	19.64	11.98
	S	32.29	33.80	34.57	34.71	34.32	34.48

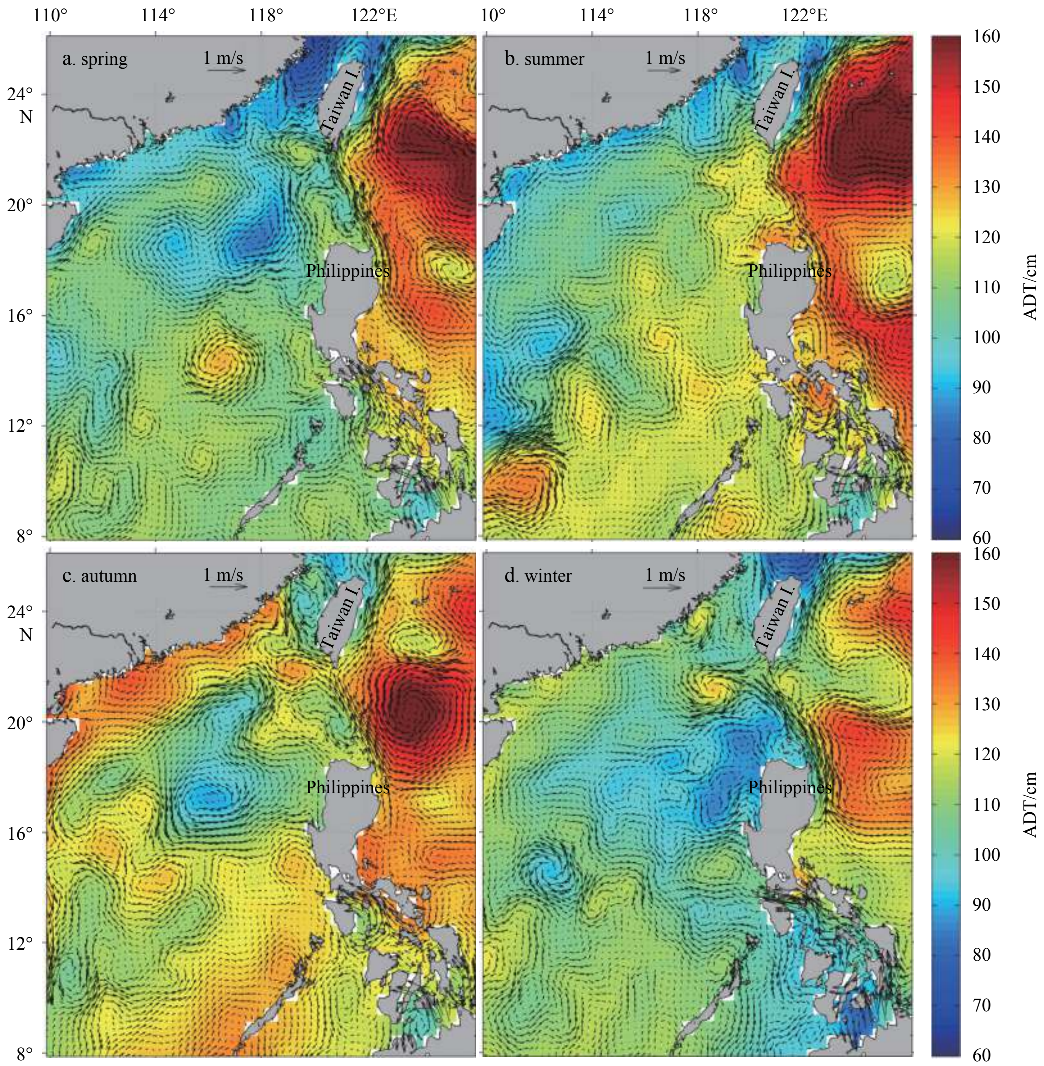

Fig. 9. Seasonal average absolute dynamic topography (ADT) and geostrophic current during the cruise period (data source from AVISO).

eddies.

(5) The surface-subsurface mixed water (SU) is distributed above 150 m, 100 m, 175 m and 100 m in four seasons, respectively.

(6) The subsurface-intermediate mixed water UI is stably distributed below 250 m. Its properties show little seasonal change.

References

Chen Shangji, Du Bing. 1990. Water masses classification of the upper layer in the equatorial western Pacific using ISODATA of fuzzy cluster. Acta Oceanologica Sinica, 9(2): 187–201

Cheng Guosheng, Sun Jiadong, Zu Tingting, et al. 2014. Analysis of water masses in the northern South China Sea in summer 2011. Journal of Tropical Oceanography (in Chinese), 33(3): 10–16

Dietrich G, Kalle K, Krauss W, et al. 1980. General Oceanography. An Introduction. 2nd ed. New York: John Wiley & Sons, 1–626

Du Chuanjun, Liu Zhiyu, Dai Minhan, et al. 2013. Impact of the Kuroshio intrusion on the nutrient inventory in the upper northern South China Sea: insights from an isopycnal mixing model. Biogeosciences, 10(10): 6419–6432, doi: 10.5194/bg-10-6419-

2013

Hu Jianyu, Zheng Quanan, Sun Zhenyu, et al. 2012. Penetration of nonlinear Rossby eddies into South China Sea evidenced by cruise data. Journal of Geophysical Research: Oceans, 117(C3): C03010, doi: 10.1029/2011JC007525

Li Lei, Li Fengqi, Su Jie, et al. 2002a. Analysis on water masses in the South China Sea in summer and winter of 1998. Oceanologia et Limnologia Sinica (in Chinese), 33(4): 393–401

Li Fengqi, Li Lei, Wang Xiuqin, et al. 2002b. Water masses in the South China Sea in summer and winter of 1998 and water exchange between the Pacific and the South China Sea. Journal of Ocean University of Qingdao (in Chinese), 32(3): 329–336

Li Fengqi, Su Yusong. 1989. Application of method of fuzzy sets to the analysis of water masses in the northern South China Sea. Journal of Ocean University of Qingdao, 19(1): 474–492

Li Fengqi, Su Yusong, Fan Liqun. 1989a. Application of method of fuzzy sets to the analysis of water masses in the northern South China Sea. Haiyang Xuebao (in Chinese), 7(2): 170–185

Li Fengqi, Su Yusong, Fan Liqun. 1989b. Discrimination analysis of water masses in the north area of the South China Sea. Journal of Ocean University of Qingdao (in Chinese), 19(1): 181–188

Li Fengqi, Su Yusong, Yu Zuxiang. 1983. A clustering analysis test in analysis of modified water masses in the shallow sea. Haiyang Xuebao (in Chinese), 5(6): 675–686

Li Fengqi, Wang Fengqin, Su Yusong. 1992. A clustering method with the fuzzy density in distinguishing water masses. Journal of Ocean University of Qingdao (in Chinese), 22(1): 12–18

Liu Changjian, Du Yan, Zhang Qingrong, et al. 2008. Seasonal variation of subsurface and intermediate water masses in the South China Sea. Oceanologia et Limnologia Sinica (in Chinese), 39(1): 55–64

Liu Zenghong, Li Lei, Xu Jianping, et al. 2001. Analysis of water masses in the South China Sea in the summer of 1998. Donghai Marine Science (in Chinese), 19(3): 1–10

Mao Hanli, Ren Yunwu, Wan Guoming. 1964. A preliminary investigation on the application of using T-S Diagrams for a quantitative analysis of the water masses in the shallow water area. Oceanologia et Limnologia Sinica (in Chinese), 6(1): 1–22

Nitani H. 1972. Beginning of the Kuroshio. In: Stommel H, Yoshida K, eds. Kuroshio, Its Physical Aspects. Tokyo: University of Tokyo Press, 129–163

Qiu Daoli, Zhou Shilai, Li Changming. 1984. A preliminary study on application of cluster analysis of water masses in the Yellow Sea Division. Haiyang Xuebao (in Chinese), 6(3): 281–292

Su Yusong, Yu Zuxiang, Li Fengqi. 1983. Application of cluster analysis method for analyzing the water-masses in the shallow water area and the analysis of modified water masses in the Huanghai Sea and the East China Sea. Oceanologia et Limnologia Sinica (in Chinese), 14(1): 1–12

Tian Tian, Wei Hao. 2005. Analysis of water masses in the northern South China Sea and Bashi Channel. Periodical of Ocean University of China (in Chinese), 35(1): 9–12, 28

Wyrtki K. 1961. Physical Oceanography of the Southeast Asian Water. In: NAGA Report Vol. 2, Scientific Result of Marine Investigation of the South China Sea and Gulf of Thailand 1959–1961, Scripps Institution of Oceanography. La Jolla, California: Scripps Institution of Oceanography, 195

Xie Lingling, Zheng Quanan, Tian Jiwei, et al. 2016. Cruise observation of Rossby waves with finite wavelengths propagating from the Pacific to the South China Sea. Journal of Physical Oceanography, 46(10): 2897–2913, doi: 10.1175/JPO-D-16-0071.1

Xie Lingling, Zheng Quanan, Zhang Shuwen, et al. 2017. The Rossby normal modes in the South China Sea deep basin evidenced by satellite altimetry. International Journal of Remote Sensing, 39(2): 399–417

Yang Dongmei, Li Fengqi, Su Yusong, et al. 1992. Fuzzy sets methods in analysis of water masses. Oceanologia et Limnologia Sinica (in Chinese), 23(3): 227–234

Zheng Quanan, Tai Changkuo, Hu Jianyu, et al. 2011. Satellite altimeter observations of nonlinear Rossby eddy-Kuroshio interaction at the Luzon Strait. Journal of Oceanography, 67: 365–376, doi: 10.1007/s10872-011-0035-2

Zheng Quanan, Xie Lingling, Zheng Zhewen, et al. 2017. Progress in research of mesoscale eddies in the South China Sea. Advances in Marine Science (in Chinese), 35(20): 131–158

Zhu Laiming, Ji Weidong. 2002. Clustering analysis of the vertical distribution of water masses in the South China Sea. Transaction of Oceanology and Limnology (in Chinese), (4): 1–6

Zou Emei, Guo Binghuo, Tang Yuxiang, et al. 2000. The hydrographic features and water masses analyses of the southern Huanghai Sea in the spring of 1996. Haiyang Xuebao (in Chinese), 22(1): 17–26